Anisotropy Assessment of Dipole Sonic Log Data through Dispersion Analysis

Thu Bui[1], *Jyoti Behura*[1,2*], *Farnoush Forghani*[1], *and Manika Prasad*[1]
[1] *Colorado School of Mines,* [2] *Seismic Science LLC*

Presenting author's email: jbehura@mines.edu

Keywords

Dipole sonic log, fractures, anisotropy, dispersion, Bakken, flexural waves.

Summary

Dispersion analysis of flexural waves in dipole sonic log can reveal the anisotropy, shear velocity, and presence of fractures within the formations adjacent to the borehole. In this study, we implement the Phase Shift method to compute the dispersion of dipole sonic log over the Bakken and its adjacent formations. We found significant differences in the shear velocities of the shale members (the Upper and Lower Bakken) versus the non-shale members (the Lodgepole, Middle Bakken, and Three Forks). We therefore, conclude that dispersion characteristics can be used for lithology identification. We also found that the existing method to analyze dispersion images based on the assumption of HTI medium with a single set of fractures is insufficient for characterizing the anisotropy of more complex fractured media.

Introduction

Modern borehole sonic data are acoustic measurements comprised of compressional, shear, Stoneley, and flexural full waveforms. Compressional, shear, and Stoneley waves are excited by a pulse of energy produced from a monopole sonic tool. Compressional and shear waves are characterized as body waves, which travel through layers of rocks. Stoneley waves are tube waves, a type of surface wave that travels along the borehole at the interface between solid and liquid (Haldorsen *et al.*, 2006).

In addition, modern sonic tools also excite flexural waves through dipole sources. In order to excite vibrations through a range of frequencies, a dipole source emits a chirp, or a frequency sweep of energy. Flexural waves are also characterized as a type of surface wave. Their motion can be visualized as the same motion produced along a tree when someone stands on the ground and shakes it (Haldorsen *et al.*, 2006). Flexural waves are dispersive and are used in dispersion analysis to characterize the anisotropy, shear velocity, and the presence of fractures. Note that while body waves exhibit intrinsic dispersion, surface waves exhibit dispersion due to the medium's heterogeneity, where frequency is inversely proportional to the velocity of wave propagation. In this study, we refer to dispersion as the heterogeneity-dependent dispersion of surface waves.

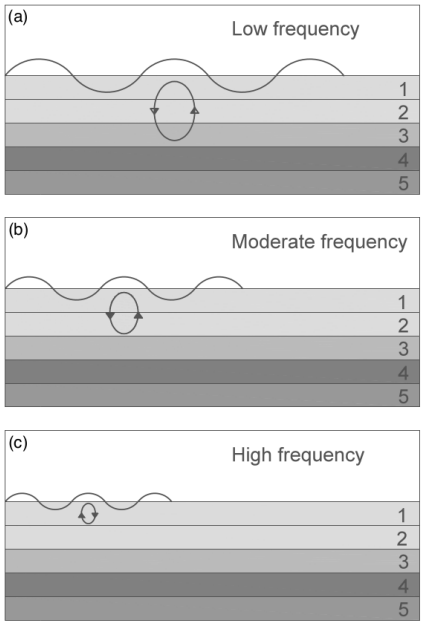

Fig. 1: a), b), and c) show simplified surface waves of a single frequency propagating along the surface of the earth, generated by three seismic sources with low, moderate, and high frequencies, respectively (figure courtesy of Olafsdottir (2014)). Each surface wave samples the subsurface at a different depth.

A wave is dispersive if its various frequency components travel with different velocities (Haldorsen *et al.*, 2006). Surface waves are generally dispersive; however, they become non-dispersive in a homogeneous isotropic medium. To understand the dispersive phenomena, we illustrate the dispersion of a simplified surface wave in Figure 1.

As shown, surface waves of different frequencies sample the subsurface at different depths. The phase velocities of surface waves depend on the elastic moduli of the layers it propagates through. Hence, each frequency component of a surface wave has a unique phase velocity. Dispersion analysis of surface waves reveals information about velocity, anisotropy and homogeneity of the medium (Olafsdottir, 2014).

In surface seismic acquisition, because of the overburden pressure, wave velocities increase with depth. It is expected that surface waves with lower frequencies are faster and have greater depth of investigation. Likewise, surface waves with higher frequencies sample the shallower subsurface and are slower. In sonic logging, the drilling process causes the sediments to be less

Dispersion Analysis of Dipole Sonic Log Data

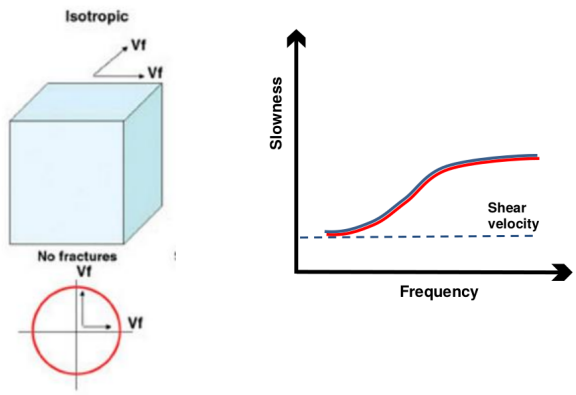

Fig. 2: Left side: Isotropic model (top cube) and shear wave velocities as a function of direction (bottom red oval) (figure courtesy of Tinnin et al. *(2008)). In isotropic media with no fractures, shear wave velocity is azimuthally invariant. Right side: As a result, the dispersion curves of two perpendicular directions (X and Y dipoles) overlap.*

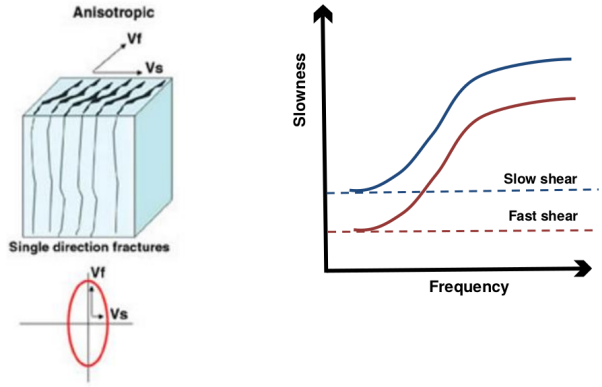

Fig. 3: Left side: Anisotropic model with a single set of fractures (top cube) and shear wave velocities as a function of direction (bottom red oval) (figure courtesy of Tinnin et al. *(2008)). In anisotropic model with a single set of fractures, shear wave velocity is strongly anisotropic. Right side: As a result, the dispersion curves of two perpendicular directions (X and Y dipoles) shows significant separation.*

compacted near the borehole. As a result, the surface wave velocities increase away from the borehole along the horizontal direction following the dispersive behavior. These characteristics can be seen in dispersion curves in Figure 2.

Franco *et al.* (2006) show that low frequency surface wave velocities approach the shear wave velocity of the virgin formation. Therefore, the low frequency part of dispersion curves provide the shear velocity of the virgin formation (shown in dashed line in Figure 2).

In a homogeneous isotropic medium with no fractures, wave velocities are the same in all directions. Therefore, we expect dispersion characteristics to be the same in all directions. As a result, the dispersion curves of the two perpendicular dipole components (X and Y) overlay, as shown in Figure 2.

In a horizontal transverse isotropic (HTI) medium with a single set of fractures, shear wave splits into fast and slow components. The shear wave with the direction of polarization parallel to the fractures travels at a higher velocity than the shear wave with the direction of polarization perpendicular to the fractures. Therefore, we expect dispersion characteristics to be different for different directions. As a result, the dispersion curves of the two perpendicular dipole components (X and Y) diverge, as shown in Figure 3.

Dispersion Analysis Methodology

Several methods are used to compute dispersion curves (Park *et al.*, 1998, 1999). We use the Phase Shift method suggested by Olafsdottir (2014) based on Park *et al.* (1998). This algorithm was chosen because of its implementation simplicity, robustness, and high accuracy. This technique involves two main steps: 1) Fourier transform and amplitude normalization, and 2) dispersion imaging. Below we describe the application of this method to our data in details:

- Step 1: Our data comprises of 13 waveforms for each perpendicular dipole orientation (X and Y). We divided the waveforms to different formation depths, where for each depth interval the waveforms are transformed from time domain into frequency domain, using Fast Fourier Transform algorithm. In the Fourier domain, the amplitudes are normalized by dividing the amplitude by its absolute value as shown:

$$\tilde{u}_{j,norm}(w) = \frac{\tilde{u}_j(w)}{|\tilde{u}_j(w)|} \tag{1}$$

, where $\tilde{u}_j(w)$ is the Fourier transform of the data, $\tilde{u}_{j,norm}(w)$ is the normalized amplitude, w is the angular frequency, and j is the receiver number, where j=1,2...n, n=13.

- Step 2: To compute the dispersion images, we select a range of possible surface wave velocities V for the formation. In our case, we chose the velocity range from 800 m/s to 3500 m/s. Using this velocity range we compute the following phase shifts

$$\phi x_j = \frac{w * (x_1 + (j-1) * \Delta x)}{V} \tag{2}$$

, where ϕx_j is the phase shift corresponding to the jth receiver, x_1 represents the distance from the source to a reference receiver, Δx is the receiver spacing. Next, using

$$\tilde{v}_{(w,V)} = \sum_{j=1}^{n} e^{-i\phi x_j} * \tilde{u}_{j,norm(w)} \tag{3}$$

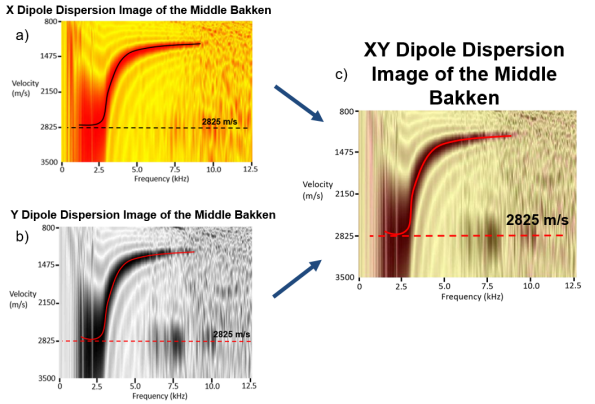

Fig. 4: a) shows X dipole dispersion image of the Middle Bakken in hot color map (highest amplitude in red), b) shows Y dipole dispersion image of the Middle Bakken in gray scale color map (highest amplitude in black), c) shows an overlay of X and Y dispersion images of the Middle Bakken with highest amplitude in dark purple. The solid lines indicate the main dispersion curves (overlap in this case) and the dashed lines indicate low frequency dispersion tail approaching the formations shear velocity. The y-axis is in decreasing velocity (m/s) and the x-axis is in increasing frequency (kHz).

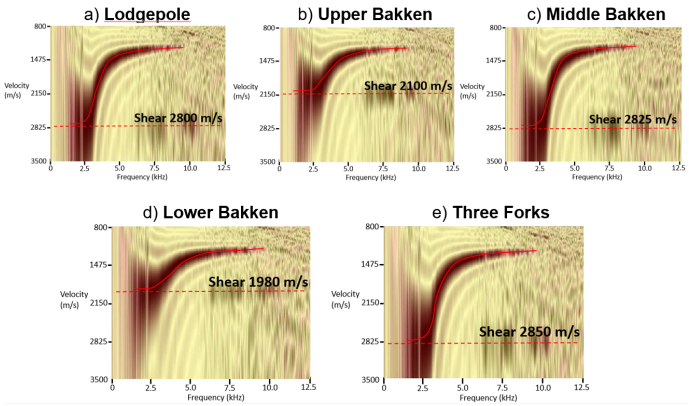

Fig. 5: a), b), c), d), and e) show the overlay dispersion images of the Lodgepole, Upper Bakken, Middle Bakken, Lower Bakken, and the underlying Three Forks, respectively. The solid lines indicate the main dispersion curves with highest amplitude in dark purple (they overlap in all studied formations). The dashed lines indicate low frequency dispersion tail approaching the formations shear velocity. The y-axis is in decreasing velocity (m/s) and the x-axis is in increasing frequency (kHz).

> we transform the data from Fourier domain to the dispersion domain (ω -V). The dispersion image exhibit high amplitudes at the actual propagating wave velocities.

In our study, we perform dispersion analysis of X and Y dipole data separately. Figure 4a and 4b illustrate two dispersion images of X and Y dipole. Figure 4c shows the overlaid dispersion image of 4a and 4b. Note that the darkest purple color represents the strongest amplitude in the overlaid dispersion images.

Analysis and Discussion

We perform dispersion analysis on multiple depths of the Lodgepole, Upper Bakken, Middle Bakken, Lower Bakken, and the underlying Three Forks. The dispersion images from the same formation are highly similar. We choose a representative dispersion image from each of these five intervals and plot them in Figure 5. Figure 5 shows dispersion images at different depths corresponding to the Lodgepole, Upper Bakken, Middle Bakken, Lower Bakken, and the underlying Three Forks. One can observe that the Upper and Lower Bakken Shale members have distinctly different dispersion characteristics than the non-shale members (the Lodgepole, the Middle Bakken and the Three Forks). For example, the shear wave velocity of non-shale members are approximately 2800 m/s compared to the shear wave velocity of shale members at approximately 2000 m/s.

Because the Bakken is heavily fractured and anisotropic (Pitman *et al.*, 2001), we expect separation between dispersion curves for this formation. However, we did not observe any separation in any of the studied formations. Although closely overlaid dispersion curves show that the above formation are all azimuthally isotropic, this result does not agree with the established findings on Bakken (Pitman *et al.*, 2001). We investigated further and learned that the interpretation method of Franco *et al.* (2006) is established based on the assumption of an HTI medium with a single set of fractures. Since the Bakken is heavily fractured by more than one fracture set (Pitman *et al.*, 2001), the interpretation from Franco *et al.* (2006) is not sufficient and cannot give insights into azimuthal anisotropy and the presence of fractures.

When the medium has more than one set of fractures, the shear wave splitting becomes more complicated. The fast and slow shear waves at certain directions can be indistinguishable from each other. As a result, dispersion curves of the two dipoles will overlay and appear as if the medium is azimuthally isotropic with no fractures. To overcome this challenge, we plan on using more azimuthal data such as cross-line dipole, performing Alford rotation, attenuation analysis, and flexural wave modeling to find the anisotropy and fracture orientation of complex fractured media.

Conclusions & Future Work

We compute dispersion images of the Bakken and its adjacent formations using the phase shift method. Our findings are as follows:

- There is significant difference in shear velocity of the shale members (the Upper and Lower Bakken) versus the non-shale members (the Lodgepole, Middle Bakken, and Three Forks). These results show that formation geology can be differentiated through dispersion analysis.
- We also found that the existing method to analyze dispersion images based on the assumption of HTI

medium with a single set of fractures is insufficient for characterizing the anisotropy of more complex fractured media.

- A new method should be developed to overcome simple fracture geometry assumptions. This will enable the use of dispersion analysis to find anisotropy and the presence of fractures in more complex fractured media.

References

Franco, JL A., Ortiz, MA M., De, G. S., Renlie, L., & Williams, S. 2006. Sonic investigation in and around the borehole. *Oilfield Review*, **18**(1), 14–33.

Haldorsen, J. BU, Johnson, D. L., Plona, T., Sinha, B., Valero, H.-P., & Winkler, K. 2006. Borehole acoustic waves. *Oilfield Review*, **18**(1), 34–43.

Olafsdottir, E. A. 2014. Multichannel Analysis of Surface Waves: Methods for dispersion analysis of surface wave data.

Park, C. B., Miller, R. D., & Xia, J. 1998. Imaging dispersion curves of surface waveson multichannel record. *Annual International Meeting Society of Exploration Geophysicists, Expanded Abstracts*, 1377–1380.

Park, C. B., Miller, R. D., & Xia, J. 1999. Multichannel analysis of surface waves. *Geophysics*, **64**(3), 800–808.

Pitman, J. K., Price, L. C., & LeFever, J. A. 2001. *Diagenesis and fracture development in the Bakken Formation, Williston Basin: Implications for reservoir quality in the middle member*. US Department of the Interior, US Geological Survey.

Tinnin, J., Hallin, J., Granath, J., & Steward, P. 2008. China case: fractured data integrated. *Geophysical Corner, AAPG Explorer*.

Acknowledgments

We thank Tom Bratton for his help with dipole sonic data and Whiting Petroleum for providing the data for this work. We also thank Azar Hasanov for his reviews and feedback.